View the Full Text HTML

JACS
A R T I C L E S

Electromechanical Phase Transition in Hexacyanometallate Nanostructure (Prussian Blue)

David Giménez-Romero,† Jerónimo Agrisuelas,‡ José Juan García-Jareño,‡,§
Joan Gregori,‡ Claude Gabrielli,† Hubert Perrot,† and Francisco Vicente*,‡

Contribution from the UPR 15 du CNRS, Laboratoire Interfaces et Systèmes Electrochimiques, Université Pierre et Marie Curie, 4 place Jussieu, 75252 Paris, France, and Departament de Química Física and Fundació General de la Universitat de València, Universitat de València, C/ Dr Moliner, 50, 46100, Burjassot, València, Spain

Received February 7, 2007; E-mail: francisco.vicente@uv.es

Abstract: This paper demonstrates the importance of the structural changeover in controlling the physical–chemical properties of hexacyanometalate-like materials (Prussian Blue). A meticulous *in situ* study of compositional variations using electroacoustic impedance techniques associated to electrogravimetric techniques in hexacyanoferrates containing K^+ alkali metals reveals the existence of a nanostructural changeover coupled to a change of the magnetic properties of these electromagnetic materials. In the same way, the electroacoustic impedance techniques can be useful both in the understanding and in the *in situ* monitoring of the structural changeovers and the magnetic behavior of all kinds of materials.

Introduction

Hexacyanometalate-like materials display a wide range of important magnetic (e.g., room-temperature magnetic ordering) and magneto-optical (e.g., ferromagnetism, photoinduced (de)-magnetization) properties.[1,2,3] These properties are associated with the flexibility of their nanostructure which allows one to improve them by selecting the appropriate electronic and magnetic configurations. The electromagnetic configurations can be tailored by external conditions, such as the magnetic field[4-6] and light,[4,7,8] and by changes in a specific local crystal environment (e.g., *in situ* electrochemical compositional variation occurring during the charge compensation imposed by a redox process[9,10]).

Traditional hexacyanometalate materials are represented by the general $M'_k[M''(CN)_6]_l \cdot mH_2O$ formula in which M' and M''

are the 3D transition metal. In this periodic nanostructure, M' is generally ascribed to the high spin metallic site, and M'', to the low spin site. The M'/M'' ratio strongly influences the electronic and spin states of hexacyanometalates containing alkali metals (e.g., Na^+, K^+, etc.). As a result, these materials tolerate different electronic spins, which limits the superexchange interactions to those across CN bridges and allows the magnetism and coloration to be changed.[2,4-6,9] Elaborate theoretical analyses suggest that the local disorder associated with the structural defects, e.g., the $\{M(CN)_6\}$ vacancies filled by $\{(H_2O)_6\}$ clusters, plays an important role in determining the photomagnetic properties.[11]

It has been shown by X-ray studies[12] that the hexacyanometalate-like materials form a face-centered cubic lattice nanostructure in which the high-spin metal and low-spin metal sites are both octahedral and surrounded by $-NC$ and $-CN$ units, with the potassium counterions and water molecules occupying the interstitial sites. Accordingly, for the established nanostructure with $k/l = 1$, the first coordination shells of M' and M'' are $\{M'(NC)_6\}$ and $\{M''(CN)_6\}$, respectively. However, for $k/l > 1$ in the general formula, some of the vacancies are filled by water molecules (or clusters), and ideally, the first coordinations of M' and M'' are, respectively, $\{M'(CN)_{6-m}m(H_2O)\}$ and $\{M''-(CN)_6\}$. In the latter case, there are two types of water molecules: (i) water molecules coordinated to M' octahedral in empty nitrogen sites and (ii) uncoordinated water molecules in interstitial positions.[11]

The valence modulation of the M' and M'' metals associated with the hexacyanometalate lattice nanostructure can easily be performed electrochemically through the different redox pro-

† Université Pierre et Marie Curie.
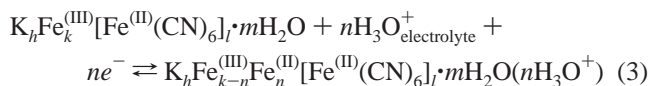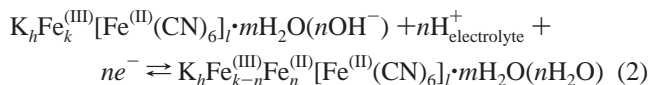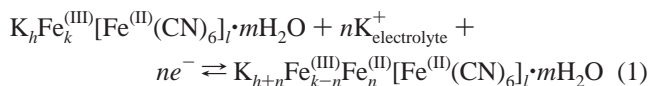‡ Departament de Química Física, Universitat de València.
§ Fundació General de la Universitat de València.

(1) Ferlay, S.; Mallah, T.; Ouahes, R.; Veillet, P.; Verdaguer, M. *Nature* **1995**, *378*, 701–703.
(2) Sato, O.; Iyoda, T.; Fujishima, A.; Hashimoto, K. *Science* **1996**, *272*, 704–705.
(3) Lescouezec, R.; Vaissermann, J.; Ruiz-Perez, C.; Lloret, F.; Carrasco, R.; Julve, M.; Verdaguer, M.; Dromzee, Y.; Gatteschi, D.; Wernsdorfer, W. *Angew. Chem., -Int. Ed*. **2003**, *42*, 1483–1486.
(4) Hayami, S.; Gu, Z.-z.; Shiro, M.; Einaga, Y.; Fujishima, A.; Sato, O. *J. Am. Chem. Soc.* **2000**, *122*, 7126–7127.
(5) Yamamoto, T.; Umemura, Y.; Sato, O.; Einaga, Y. *J. Am. Chem. Soc.* **2005**, *127*, 16065–16073.
(6) Champion, G.; Escax, V.; Cartier dit Moulin, C.; Bleuzen, A.; Villain, F.; Baudelet, F.; Dartyge, E.; Verdaguer, M. *J. Am. Chem. Soc.* **2001**, *123*, 12544–12546.
(7) Sato, O.; Iyoda, T.; Fujishima, A.; Hashimoto, K. *Science* **1996**, *271*, 49–51.
(8) Sato, O.; Kawakami, T.; Kimura, M.; Hishiya, S.; Kubo, S.; Einaga, Y. *J. Am. Chem. Soc.* **2004**, *126*, 13176–13177.
(9) Gimenez-Romero, D.; Bueno, P. R.; Garcia-Jareno, J. J.; Gabrielli, C.; Perrot, H.; Vicente, F. *J. Phys. Chem. B* **2006**, *110*, 2715–2722.
(10) Itaya, K.; Akahoshi, H.; Toshima, S. *J. Electrochem. Soc.* **1982**, *129*, 1498.

(11) Herren, F.; Fischer, P.; Ludi, A.; Halg, W. *Inorg. Chem.* **1980**, *19*, 956.
(12) Keggin, J. F.; Miles, F. D. *Nature* **1936**, *137*, 577.

cesses of these materials.[9] This control is traditionally recognized as an *in situ* metal alkali compositional change where the M′/M″ atomic composition ratio varies according to the electrochemical potential. Depending on the potential, ions are exchanged between the hexacyanometalate nanostructure and the solution to compensate the charge lost or gained by the nanostructure during the different redox processes of these materials, leading to a potential-controlled compositional variation. In the Prussian Blue (PB, a subclass of hexacyanoferrate), the modulation of the M′/M″ ratio can be described as follows:[9]

$$K_h Fe_k^{(III)}[Fe^{(II)}(CN)_6]_l \cdot mH_2O + nK_{electrolyte}^+ + \\ ne^- \rightleftharpoons K_{h+n}Fe_{k-n}^{(III)}Fe_n^{(II)}[Fe^{(II)}(CN)_6]_l \cdot mH_2O \quad (1)$$

$$K_h Fe_k^{(III)}[Fe^{(II)}(CN)_6]_l \cdot mH_2O(nOH^-) + nH_{electrolyte}^+ + \\ ne^- \rightleftharpoons K_h Fe_{k-n}^{(III)}Fe_n^{(II)}[Fe^{(II)}(CN)_6]_l \cdot mH_2O(nH_2O) \quad (2)$$

$$K_h Fe_k^{(III)}[Fe^{(II)}(CN)_6]_l \cdot mH_2O + nH_3O_{electrolyte}^+ + \\ ne^- \rightleftharpoons K_h Fe_{k-n}^{(III)}Fe_n^{(II)}[Fe^{(II)}(CN)_6]_l \cdot mH_2O(nH_3O^+) \quad (3)$$

where the $K_h Fe_k[Fe(CN)_6]_l \cdot mH_2O$ (PB) is reversibly converted to $K_{h+n}Fe_{k-n}Fe_n[Fe(CN)_6]_l \cdot mH_2O$ (known as Everitt's Salt or ES). Thus, the amount of exchanged ions can be controlled by an ne^- modulation and hence by the potential.

Two types of K^+ sites exist during this compositional control. One type of site is adjacent to the $Fe'(CN)_{6-m}m(H_2O)$ vacancies and is preferentially occupied while the other type suffers repulsive interaction.[13] During the compositional changes, K^+ must preferentially fill sites adjacent to $Fe'(CN)_{6-m}m(H_2O)$ vacancies in the structure that are formed during the $K_h Fe_k[Fe(CN)_6]_l \cdot mH_2O$ stabilization process. Thus, when all sites of the first type are occupied, which represent a fraction of about 25%, the next possibility is the occupation of the K^+ sites of the nanostructure not adjacent to $Fe'(CN)_{6-m}m(H_2O)$.[13]

The main goal of this paper is to demonstrate the structural changeover that occurs *in situ* during the alkali metal composition modulation due to the redox processes of the hexacyanoferrate nanostructure. It is associated with a change of certain physical−chemical properties of these electromagnetic materials, such as their mechanical or magnetic properties. For that purpose, electroacoustic impedance techniques associated with electrogravimetric techniques were employed.

Experimental Section

The compositional changes in response to an electrochemical modulation were carried out in a typical electrochemical three-electrode cell. The $KFe^{(III)}[Fe^{(II)}(CN)_6] \cdot mH_2O$ hexacyanoferrates were deposited on 25 mm² diameter gold electrodes of a quartz crystal (Matel−Fordahl) of a fast-response microbalance. A platinum plate was used as the counter electrode and the Ag|AgCl|KClₛₐₜ electrode was used as the reference electrode. The compositional variations were modulated by controlled changes in the charge and mass of $KFe^{(III)}[Fe^{(II)}(CN)_6] \cdot mH_2O$ (PB established formula) through an AUTOLAB potentiostat-galvanostat (PGSTAT302) and an Electrochemical Quartz Crystal Microbalance (EQCM, RQCM, Maxtek, Inc.). The electrolyte used in all the experiments was 0.50 M KCl (A. R., R. P. NORMAPUR) with a pH of about 3.06. The $KFe^{(III)}[Fe^{(II)}(CN)_6] \cdot mH_2O$ hexacyanoferrate deposit was sufficiently thin to ensure a precise relationship between

the frequency variation of the quartz crystal and the mass change without any viscoelastic artifacts. Details are given in ref 14.

To monitor the structural variation of $KFe^{(III)}[Fe^{(II)}(CN)_6] \cdot mH_2O$ by means of acoustic fundaments, the RQCM utilizes an internal phase lock oscillator referred to as a voltage controlled oscillator to drive the quartz crystal. The crystal current is monitored and the frequency of the oscillator is adjusted until there is zero phase between the crystal voltage and current. At this point, the magnitude of the current is directly proportional to the crystal conductance. This current is monitored by the RQCM and displayed as motional resistance.[15] The interaction of the piezoelectric layer with an external magnetic field was realized by means of the approximation of a magnet to an electrode of quartz crystal in air and at a distance of about 1 mm.

The setup of the electroacoustic measurements at steady-state conditions was based on a classical network analyzer (HP 4194A). All the experimental measurements were computer-controlled through homemade software HP-VEE language. All the electrical admittance was automatically performed using a 10 mV perturbation signal at 201 frequencies around the resonance frequency. Electrical admittance measurements were performed after 1 min of stabilization at each potential.

$KFe^{(III)}[Fe^{(II)}(CN)_6] \cdot mH_2O$ was electrochemically deposited on a gold electrode of the quartz crystal by immersion in 0.02 M $K_3Fe(CN)_6$ (A.R., Panreac), 0.02 M $FeCl_3$ (Sigma) and 0.01 M HCl (A. R., R. P. NORMAPUR™) solution. A controlled cathodic current of 40 $\mu A \cdot cm^{-2}$ was applied for 150 s or 250 s (the films of 250 s were used only during the measurements realized at steady-state conditions) to obtain $Fe_4^{(III)}[Fe^{(II)}(CN)_6]_3 \cdot mH_2O$. After this deposition, the $KFe^{(III)}[Fe^{(II)}(CN)_6] \cdot mH_2O$ nanostructure was generated in several voltammetric cycles [0.6, −0.25] V in 0.50 M KCl with a pH of 3.06, according to refs 16−18.

Results and Discussion

The thickness shear mode resonators have been successfully used as gravimetric sensors by using the Sauerbrey relation between the resonant frequency and added mass[19] (often referred to as a quartz crystal microbalance (QCM)), which reach the subnanogram level.[20] However, in addition to the mass of the film coating the resonator, other factors such as its viscoelasticity, the solution properties, and temperature contribute to the electroacoustic behavior of the loaded piezoelectric crystal.[21] The interactions with the coating or/and solution cause changes in the quartz resonance characteristics which can be studied from the measurement of the resonant frequency of the crystal and completed by means of electroacoustic techniques.

The acoustic behavior of a quartz resonator loaded with a thin layer can be described in terms of a Butterworth−Van Dyke (BVD) equivalent circuit model.[22] The elements in this model are related to the physical properties of the crystal, the coating, and the solution. The equivalent circuit is constituted by a "motional" arm, incorporating three elements in series (a resistance R_m, an inductance L_m, and a capacitance C_m) which is in parallel with a "static" arm including a capacitance, C_s.

(13) Bueno, P. R.; Gimenez-Romero, D.; Gabrielli, C.; Garcia-Jareno, J. J.; Perrot, H.; Vicente, F. *J. Am. Chem. Soc.* **2006**, *128*, 17146−17152.

(14) Garcia-Jareño, J. J.; Gabrielli, C.; Perrot, H. *Electrochem. Commun.* **2000**, *2*, 195−200.
(15) *Operation and service manual of RQCM*, 2nd ed. (Maxtek Inc.).
(16) Garcia-Jareño, J. J.; Sanamatias, A.; Vicente, F.; Gabrielli, C.; Keddam, M.; Perrot, H. *Electrochim. Acta* **1998**, *45*, 3765−3776.
(17) Mortimer, R. J.; Rosseinsky, D. R. *J. Electroanal. Chem.* **1983**, *151*, 133.
(18) Mortimer, R. J.; Rosseinsky, D. R. *J. Chem. Soc., Dalton Trans.* **1984**, *9*, 2059.
(19) Sauerbrey, G. *Z. Phys.* **1959**, *155*, 206.
(20) Lucklum, R.; Hauptmann, P. *Electrochim. Acta* **2000**, *45*, 3907−3917.
(21) Muramatsu, H.; Tamiya, E.; Karube, I. *Anal. Chem.* **1988**, *60*, 2142.
(22) Parzen, B. *Design of Crystal and Other Harmonic Oscillators*; Wiley, New York, 1983.

It is well-known that the electrical model can be converted to a mechanical model by means of the electromechanical coupling factor as an electromechanical analogy.[21] Thus, the motional resistance (R_m) represents the energy dissipation due to the internal friction and damping from the crystal mounting. L_m is the initial mass/motional inertia of the system, C_m is the mechanical elasticity of the quartz, and C_s consists of the capacitance of the quartz between the electrodes and the parasitic capacitance of the crystal fixture.

In a detailed model, the loaded resonator is a combination of a quartz crystal with two electrodes and a film deposited on them. Accordingly, Granstaff et al.[23] have deduced a relation between the mechanical properties of the different components of this piezoelectric system and the impedance of the "motional" arm of the BVD equivalent circuit model, Z_m:

$$Z_m = j\frac{\omega\rho_{film}\,d_{film}\,d_{quartz}^2}{4e_{26}^2 A}\tanh\left(j\omega\,\sqrt{\frac{\rho_{film}}{G_{film}}}d_{film}\right) +$$
$$\frac{d_{quartz}^2}{4e_{26}^2 A}\sqrt{j\omega\rho_{solution}\eta_{solution}} + \frac{\pi^2\eta_{quartz}\,d_{quartz}}{8\,K^2 c_{66}\xi_{22}A} \quad (4)$$

where $j = \sqrt{-1}$, d is the layer thickness, ρ is the mass density, ω is the angular frequency, η is the viscosity, and G is the complex shear modulus. K^2 is the electromechanical coupling factor for no loss quartz (7.74×10^{-3} [23]), η_{quartz} is the effective viscosity of quartz (3.5×10^{-4} kg m^{-1} s^{-1} [23]), c_{66} is the piezoelectrically stiffened elastic constant for no loss quartz (2.947×10^{10} N m^{-2} [23]), ξ_{22} is the quartz permittivity (3.982×10^{-11} A^2 s^4 kg^{-1} m^{-3} [23]), e_{26} is the piezoelectric stress constant for quartz (95.3×10^{-3} A s m^{-2} [23]), and A is the active electrode area.

By considering that the film thickness is very thin, the motional resistance of the BVD equivalent circuit can be related easily to the physical parameters of the quartz, the film, and the solution through the real part of eq 4. This relation corresponds to

$$R_m = \frac{\pi^2\eta_{quartz}d_{quartz}}{8K^2 c_{66}\xi_{22}A} + \frac{d_{quartz}^2}{4e_{26}^2 A}\left(\frac{\omega^2\rho_{film}^{3/2}d_{film}^2 G'_{film}}{(G''_{film})^2 - (G'_{film})^2}\right) +$$
$$\frac{d_{quartz}^2}{4e_{26}^2 A}\sqrt{\frac{\omega\rho_{solution}\eta_{solution}}{2}} \quad (5)$$

where the complex shear modulus of the film is equal to $G'_{film} + jG''_{film}$. It is important to emphasize that the term $(G''_{film})^2 - (G'_{film})^2$ is always positive with respect to the applied potential for the $K_hFe_k[Fe(CN)_6]_l \cdot mH_2O$ materials.[14] So, an increase of the physical parameters of the film implies the increase of the motional resistance. As a result, the motional resistance allows structural changeovers to be monitored *in situ* during the alkali metal composition modulation of the hexacyanoferrate nanostructure since the solution and quartz physical parameters are kept constant during this modulation. This technique can be also applied to other materials.

Figure 1 shows the voltammetric scan (Figure 1a) and the motional resistance change (Figure 1b) measured on the $K_hFe_k[Fe(CN)_6]_l \cdot mH_2O$ material, synthesized as explained

(23) Granstaff, V. E.; Martin, S. J. *J. Appl. Phys.* **1994**, *75*, 1319.
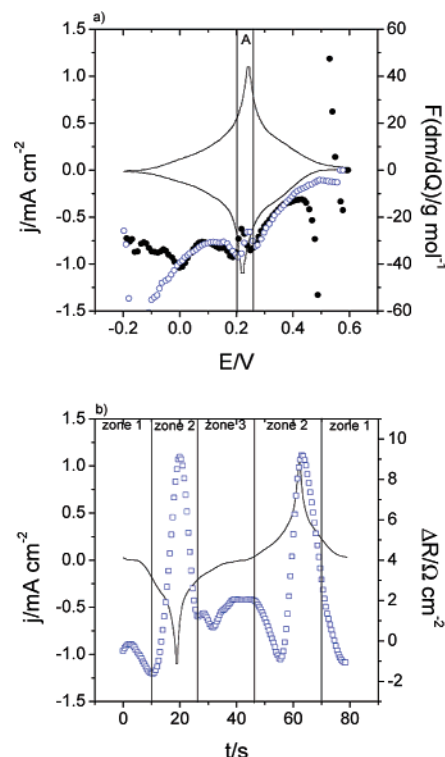
Figure 1. Voltammetric scan (solid line) of $K_hFe_k[Fe(CN)_6]_l \cdot mH_2O$ material and that previously stabilized in the electrolytic environment. The electrolyte was 0.50 M KCl in a pH of about 3.06. (a) $F(dm/dQ)$ function here is represented during the cathodic compositional variation (insertion, (●)) and during the anodic compositional variation (deinsertion, (○)). (b) The evolution of the motional resistance here is represented during the full voltammetric scan (□).

in the literature.[9,24] $K_hFe_k[Fe(CN)_6]_l \cdot mH_2O$ is commonly referred to as the soluble PB which is reversibly converted to $K_{h+n}Fe_{k-n}Fe_n[Fe(CN)_6]_l \cdot mH_2O$ during the compositional variation with respect to the K$^+$ insertion, eqs 1−3. During this redox process, the motional resistance provides direct information on the structural changes (coating thickness, density, and/or complex shear modulus) of the nanostructured matrix, eq 5.

An increase of 2 Ω cm^{-2} in the motional resistance is observed between the PB form (zones 1, Figure 1b) and the ES form (zones 3, Figure 1b) of the hexacyanoferrate matrix, which corresponds to a $|\Delta f/\Delta R_m|$ experimental ratio of 250 Hz Ω^{-1}. This ratio is significantly larger than 10 Hz Ω^{-1}, which is the characteristic value of a net viscoelastic effect.[25] Hence this ratio demonstrates that the viscoelastic effects on hexacyanoferrate matrix are negligible during the alkali metal composition modulation, as was demonstrated in a previous paper for films acoustically thin enough.[14]

Developing the BVD equivalent circuit model and as it is observed in eq 5, the motional resistance is the addition of three different terms: the resistances related to the properties of the quartz crystal, the electrolyte, and the film. Consequently and considering eq 5, the increase of the motional resistance between the PB structure and the ES structure is equivalent to

(24) Rosseinsky, D. R. J.; Glasser, L.; Jenkins, H. D. B. *J. Am. Chem. Soc.* **2004**, *126*, 10472−10477.
(25) Martin, S. J.; Granstaff, V. E.; Frye, G. C. *Anal. Chem.* **1991**, *63*, 2272.

$$\frac{R_m^{ES} - R_m^{PB}}{R_m^{PB} - R_R} =$$

$$\frac{(\rho_{ES})^{3/2}(d_{ES})^2 \dfrac{G'_{ES}}{(G''_{ES})^2 - (G'_{ES})^2} - (\rho_{PB})^{3/2}(d_{PB})^2 \dfrac{G'_{PB}}{(G''_{PB})^2 - (G'_{PB})^2}}{(\rho_{PB})^{3/2}(d_{PB})^2 \dfrac{G'_{PB}}{(G''_{PB})^2 - (G'_{PB})^2}}$$

(6)

where R_R is the motional resistance due to the three-layer composite resonator (piezoelectric material and its corresponding electrodes).

Accordingly, if the PB structure is the same as the ES structure as it is considered in literature,[12,26] ($G'_{PB} = G'_{ES}$, $G''_{PB} = G''_{ES}$ and $d_{PB} = d_{ES}$), then eq 6 can be simplified,

$$\frac{R_m^{ES} - R_m^{PB}}{R_m^{PB} - R_R} = \frac{(m_{ES})^{3/2} - (m_{PB})^{3/2}}{(m_{PB})^{3/2}}$$

(7)

where m_i is the mass of the i film.

The experimental variation of the motional resistance during the compositional modulation of the hexacyanoferrate material is close to 4%, whereas the variation percentage of the gained mass for the structure during this modulation is close to 11% (both values were calculated experimentally). Thus, these values are in disagreement with eq 7, and consequently, the increase of the motional resistance between the PB structure and the ES structure (i.e., between zone 1 and 3, Figure 1b) cannot be explained only by the increase of the film density.

On the other hand, in zones 2 of Figure 1b, the evolution of the motional resistance with respect to the compositional modulation of the hexacyanoferrate material does not agree with the evolution of the film density established by eq 5 (there is an inexplicable maximum during this compositional modulation due to the different redox processes of this material). Besides, the zones 2 of Figure 1b also cannot be explained only by means of a simple transition between two structures, which would impose different stresses on the quartz crystal, as it would lead to a continuous change of the motional resistance.

Some authors, as Muramatsu et al.,[21] relate alternatively the motional resistance to the rheological properties of the loading solution. As eqs 1−3 show, the rheological properties of the solution at the interface film/solution change depending on the sense of the compositional modulation owing to the different movement of the ionic species. In view of that, the zones 2 of Figure 1b cannot be explained by means of the rheology of the loading solution since a similar evolution of motional resistance is recorded in both compositional modulation senses (opposite ionic flux between the solution and the film depending on the sense of this modulation).

On the other hand, Garcia-Jareño et al.[27] have shown that the electrical conductance of this material is maximum in the maximum of the compositional modulation (zones 2 in Figure 1b). Nonetheless, the conductance in the maximum of this modulation should be minimum considering an inverse relation
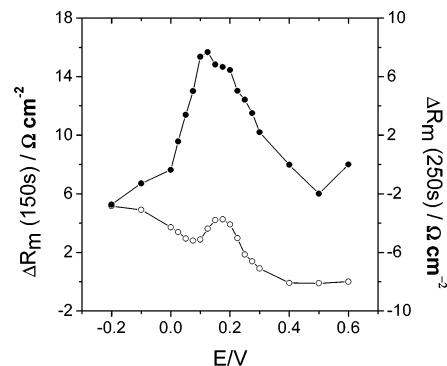
Figure 2. Evolution of the motional resistance calculated at steady-state conditions. Data of $K_hFe_k[Fe(CN)_6]_l \cdot mH_2O$ material deposited applying a controlled cathodic current of 40 $\mu A \cdot cm^{-2}$ (○) during 150 s and (●) during 250 s.

between the conductance and the motional resistance.[28] Accordingly, the motional resistance evolution also cannot be explained by means of the conductance parameters.

To explain the evolution of the motional resistance in zones 2 of Figure 1b, kinetic aspects can also be discarded since similar results were also obtained in steady-state conditions (Figure 2). The zones 2 of Figure 1b cannot be explained by means of viscoelastic effects as well, since the experimental $|\Delta f/\Delta R_m|$ ratio tends to infinity in this potential interval and, furthermore, the theoretical and experimental differential mass sensitivities given by the Sauerbrey equation are indistinguishable for these materials.[14] As a result, the evolution of the motional resistance during the compositional modulation of the hexacyanoferrate material (zones 2 in Figure 1b) can be only explained through a variation of the physical properties of the structure of these electromagnetic materials. This is supported by the fact that the maximum of the motional resistance increases proportionally with the film quantity deposited on the quartz resonator (Figure 2).

Among these physical properties, it is known that the magnetic properties of these materials are tunneled by the atomic composition ratio of (high spin metallic sites)/(low spin metallic sites).[2,7] The interaction between an external magnetic field and a dielectric material (e.g., a quartz resonator) may be evidenced by the piezoelectric distortion.[29,30] Besides, this interaction has been taken advantage of to devise magnetic field sensors.[31,32] Figure 3 shows that, for a quartz resonator in air, the motional resistance increases when the piezoelectric system is under the influence of an external magnetic field. Accordingly, the sharp change of the motional resistance of the quartz crystal loaded by PB can be considered as directly related to the modification of the magnetic properties (coercive field) of the Prussian Blue-like materials (zones 2 in Figure 1b). The change of the motional resistance during a conventional compositional modulation due to a redox process may reveal the variation of the coercive field associated with these electromagnetic materials. Thus, Figure

(26) Ayers, J. B.; Waggoner, W. H. *J. Inorg. Nucl. Chem.* **1971**, *3*3, 721.
(27) Garcia-Jareño, J. J.; Sanamatias, A.; Navarro-Laboulais, J.; Benito, D.; Vicente, F. *Electrochim. Acta* **1998**, *43*, 235−243.

(28) Xie, Q. J.; Zhang, Y. Y.; Yuan, Y.; Guo, Y. H.; Wang, X. J.; Yao, S. *J. Electroanal. Chem.* **2000**, *484*, 41−54.
(29) Ueda, K.; Saeki, H.; Tabata, H.; Hawai, T. *Solid State Commun.* **2000**, *116*, 221−224.
(30) Fiebig, M.; Lottermösser, T.; Fröhlich, D.; Goltsev, A. V.; Pisarev, R. V. *Nature* **2002**, *419*, 818−820.
(31) Fetisov, Y. K.; Bush, A. A.; Kamentsev, K. E.; Ostashchenko, A. Y.; Srinivasan, G. *IEEE Sens. J.* **2006**, *6*, 935−938.
(32) Wood, V. E.; Austin, A. E. In *Proceedings of the Symposium on Magnetoelectric Interaction Phenomena in Crystals, Seattle, 1973*; Freeman, A. J., Schmid, H., Eds.; Gordon & Breach: New York, 1975; pp 181.
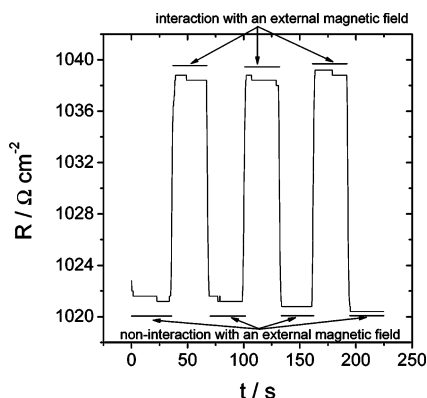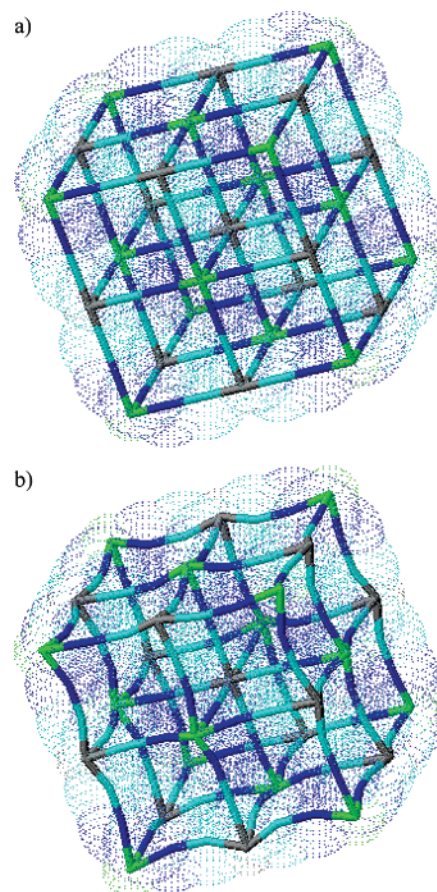
Figure 3. Influence of an external magnetic field on the measured motional resistance of a quartz resonator in air.

1b and Figure 2 are in agreement with Sato et al.[7] who have previously established that the coercive field is different for the structures of the PB and ES analogues. Therefore, the maximum of the motional resistance observed in zones 2 of Figure 1b can be explained by the change of magnetic field of the Prussian Blue-like materials. Accordingly, this maximum corresponds to an Fe^{3+}/Fe^{2+} ratio close to 0.40, which was determined by Ohkoshi et al.[33] for the maximum of the coercive field in PB analogues.

The X-ray powder-diffraction spectrum for the Ohkoshi ratio indicates that the modification of the magnetic properties is related to the variation of the lattice constant.[33] Accordingly, the evolution of the motional resistance during the alkali metal composition modulation is also related to the structural changeover, already shown in a previous paper.[13] This structural changeover is in concordance with the two types of K^+ sites which exist during this compositional control.[13] The one is localized adjacent to $Fe'(CN)_{6-m}m(H_2O)$ vacancies, while the other suffers a repulsive interaction and is occupied from about the Ohkoshi ratio. Thus, both types would correspond to the different sites occupied by the K^+ ions in the PB and ES structures, respectively.

Results reported in the literature for the temperature-induced phase transition of hexacyanometalate-like materials indicate that the unit cell volume of the lattice of the high-temperature phase (about 300 K) is reduced by about 10% in the low-temperature phase (about 160 K).[34] This cell contraction starts locally and spreads homogeneously in the solid without loss of crystallinity[35] owing to the shortening of the metal–ligand bond accompanying the divalent metal (high spin) to the trivalent metal (low spin) transformation.[36] The structural change spreads in a cooperative way in the whole solid. This is possible thanks to the flexibility of the metal–NC angle in the metal–NC–Fe entities and by the swing of the metal and Fe coordination polyhedron.[36]

Analogous to the temperature-induced phase transition, the ne^- modulation occurring during a redox process controls the oxidation state of the metal coordinated to the –NC ligand, eqs 1–3. Subsequently, the change of the coordination sphere

(33) Ohkoshi, S.; Iyoda, T.; Fujishima, A.; Hashimoto, K. *Phys. Rev. B* **1997**, *56*, 11642–11652.
(34) Ohkoshi, S.; Tokoro, H.; Hashimoto, K. *Coord. Chem. Rev.* **2005**, *249*, 1830–1840.
(35) Escax, V.; Bleuzen, A.; Itie, J. P.; Munsch, P.; Varret, F.; Verdaguer, M. *J. Phys. Chem. B* **2003**, *107*, 4763–4767.
(36) Bleuzen, A.; Escax, V.; Ferrier, A.; Villain, F.; Verdaguer, M.; Munsch, P.; Itie, J. P. *Angew. Chem., Int. Ed.* **2004**, *43*, 3728–3731.

Figure 4. (a) Structure of Prussian Blue hexacyanoferrate. (b) ES crystalline structure proposed theoretically. It is believed that the vacancies in the Fe'-$(CN)_6$ site are surrounded by water molecules ($Fe'(CN)_{6-m}m(H_2O)$ sites), whose stoichiometry is very difficult to be determined. Interstitial alkali metals were omitted for clarity. Green sticks correspond to Fe(III) atoms, black sticks correspond to Fe(II) atoms, blue sticks correspond to nitrogen atoms, and cyan sticks correspond to carbon atoms.

of the metal linked to the –NC ligand caused by the variation of the oxidation state of this metal explains the structural changeover detected by means of the motional resistance during this transformation. The Fe linked to the –NC ligand in the Prussian Blue structure is stable in its trivalent oxidation state, reducing this state to divalent during the ne^- modulation inversely to temperature-induced phase transition.[34,36]

Hence, the transition between the PB and ES structures must involve the increase of the unit cell volume owing to the transformation of a cubic structure (PB established structure) in a tetragonal structure (the ES structure proposed in Figure 4 of this paper considering the structure of the PB analogues at high temperatures). This volume increase is due to the lengthening of the Fe–NC bond accompanying the Fe(III) → Fe(II) transformation during the ne^- modulation. In this way, this bond lengthening explains easily the entrance of a hydrated proton from the compositional change of K^+ ions implied in zones 2 of Figure 1b, as commented on in a previous paper.[9] This structural changeover also easily explains the global variation of the motional resistance between the PB and ES structures given that a volume increase of about 5% (similar to the volume increase established by Ohkoshi et al.[34] for PB analogues), together with the mass increase measured between both structures, involves a variation of the motional resistance between both structures of about 4% (this value is the

experimental variation of the motional resistance established previously for this transition).

The tetragonal structure of the PB derivatives presents two important characteristics: it is more rigid than the cubic structure,[36] and it implies an increase of the coercive field.[34] That is in agreement with the higher stiffness showed by the ES structure. Furthermore, the cubic/tetragonal transformation explains straightforwardly the increase of the coercive field in the reduced states of the PB analogues.[7]

The variation of the coercive field explains also the strange narrow voltammetric peak of the hexacyanometalate-like materials (Figure 1) given that the variation of this field during the ne^- modulation induces necessarily an extra current. This additional current originates the decrease of the $F(dm/dQ)$ function in zone A of Figure 1a ($F(dm/dQ)$ function allows the molecular weight of the exchanged species between the solution and the electrode to be determined from Faraday's law[9,37]) since there is an extra current nonassociated with an ionic exchange to reach the material electroneutrality during this redox process. In steady-state conditions,[38] the decrease of the $F(dm/dQ)$ function also takes place but to a lesser extent, corroborating the apparition of an extra current due to the modulation of the coercive field. So, this new current explains the fact that the voltammetric and mass evolution of these materials cannot be explained by considering only the three electrochemical processes associated with the ne^- modulation of the PB structure and related to K^+,[9,39] H^+,[9,39] and H_3O^+ [9] exchange, as shown in eqs 1–3.

The contribution to the electric current of the generated magnetic field for these materials can be easily estimated from the $F(dm/dQ)$ function. Thus, this extra current is equivalent to about 40% of the total current during the sudden electric activation of the hexacyanoferrate-like materials (zones 2 in Figure 1b). In a forward-looking approach, the sudden electric activation of the hexacyanoferrate-like materials observed in zones 2 of Figure 1b could be employed in electronic devices.
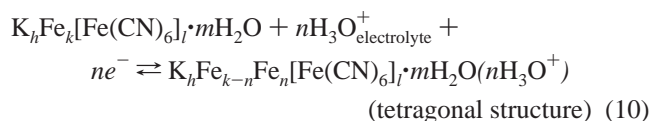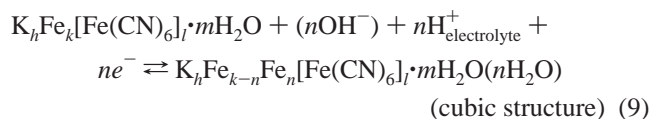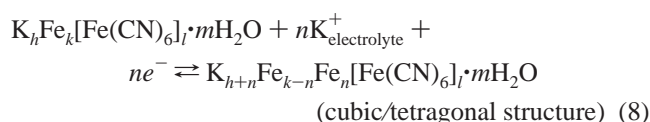
Finally, this structural changeover justifies the decrease of the adherence to the substrate of the hexacyanoferrate material observed experimentally during the PB/ES transformation. Summarizing, all theses concordances validate the structure changeover as well as the ES structure proposed in this paper (Figure 4). Thus, the difference between the motional resistance of the PB and ES structures is easily explained as the sum of two different contributions: a contribution due to a structural changeover and a magnetic contribution induced by this changeover. Consequently, the electroacoustic techniques by means of the motional resistance allow, probably for the first time, structural changeovers and magnetic behavior of the hexacyanoferrate nanostructure to be monitored *in situ* during the alkali metal composition modulation (an electrochemical− magnetic phase transition).

Conclusion

A structural changeover in hexacyanometalate material was found to be a determinant in explaining the strong changes observed in the properties of hexacyanometalates (electrical, optical, and magnetic) during the alkali metal composition modulation of their nanostructure. During this modulation, the unit cell changes its structural configuration of a cubic structure (PB established structure, Figure 4a) into a tetragonal structure (ES structure proposed in this paper, Figure 4b).

Accordingly, eqs 1−3 can be rewritten as

$$K_h Fe_k[Fe(CN)_6]_l \cdot mH_2O + nK^+_{electrolyte} +$$
$$ne^- \rightleftarrows K_{h+n}Fe_{k-n}Fe_n[Fe(CN)_6]_l \cdot mH_2O$$
$$\text{(cubic/tetragonal structure) (8)}$$

$$K_h Fe_k[Fe(CN)_6]_l \cdot mH_2O + (nOH^-) + nH^+_{electrolyte} +$$
$$ne^- \rightleftarrows K_h Fe_{k-n}Fe_n[Fe(CN)_6]_l \cdot mH_2O(nH_2O)$$
$$\text{(cubic structure) (9)}$$

$$K_h Fe_k[Fe(CN)_6]_l \cdot mH_2O + nH_3O^+_{electrolyte} +$$
$$ne^- \rightleftarrows K_h Fe_{k-n}Fe_n[Fe(CN)_6]_l \cdot mH_2O(nH_3O^+)$$
$$\text{(tetragonal structure) (10)}$$

A careful and detailed analysis of acoustic techniques revealed that the maximum compositional modulation of these materials involves a parasitic current due to the generation of a coercive field. The approach described here sheds light on the mechanism involved in electrochemical tunable magnetic phase transition. Consequently, the acoustic techniques by means of the motional resistance allow us to monitor *in situ*, probably for the first time, the structural changeover and magnetic behavior of the hexacyanoferrate nanostructure during the alkali metal composition modulation which can be extensive to other materials.

(37) Gimenez-Romero, D.; Garcia-Jareno, J. J.; Vicente, F. J. *Electroanal. Chem.* **2003**, *558*, 25−33.
(38) Gimenez-Romero, D.; Bueno P. R.; Gabrielli C.; Garcia-Jareno J. J.; Perrot H.; Vicente F. *J. Phys. Chem. B* **2006**, *110*, 19352−19363.
(39) Garcia-Jareño, J. J.; Sanamatias, A.; Navarro-Laboulais, J.; Vicente, F. *Electrochim. Acta* **1998**, *44*, 395−405.